

Cite this: *Chem. Sci.*, 2015, 6, 1754

# A facile route to electronically conductive polyelectrolyte brushes as platforms of molecular wires†

Karol Wolski, Michał Szuwarzyński and Szczepan Zapotoczny\*

A facile strategy for the synthesis of conjugated polyelectrolyte brushes grafted from a conductive surface is presented. Such brushes form a platform of molecular wires oriented perpendicularly to the surface, enabling efficient directional transport of charge carriers. As the synthesis of conjugated polymer brushes using chain-growth polymerization *via* a direct “grafting from” approach is very challenging, we developed a self-templating surface-initiated method. It is based on the formation of multimonomer template chains in the first surface-initiated polymerization step, followed by the second polymerization leading to conjugated chains in an overall ladder-like architecture. This strategy exploits the extended conformation of the surface-grafted brushes, thereby enabling alignment of the pendant polymerizable groups along the template chains. We synthesized a new bifunctional monomer and used the developed approach to obtain quaternized poly(ethynylpyridine) chains on a conductive indium tin oxide surface. A catalyst-free quaternization polymerization was for the first time used here for surface grafting. The presence of charged groups makes the obtained brushes both ionically and electronically conductive. After doping with iodine, the brushes exhibited electronic conductivity, in the direction perpendicular to the surface, as high as  $10^{-1}$ – $10^0$  S m<sup>-1</sup>. Tunneling AFM was used for mapping the surface conductivity and measuring the conductivity in the spectroscopic mode. The proposed synthetic strategy is very versatile as a variety of monomers with pendant polymerizable groups and various polymerization techniques may be applied, leading to platforms of molecular wires with the desired characteristics.

Received 31st December 2014

Accepted 12th January 2015

DOI: 10.1039/c4sc04048a

www.rsc.org/chemicalscience

## Introduction

Since the first synthesis of polyacetylene<sup>1</sup> a rapid development of conjugated polymers has been observed. Non-doped conjugated polymers are semiconductors and find applications, *e.g.*, in organic light emitting diodes,<sup>2</sup> field-effect transistors<sup>3</sup> and as active layers in organic solar cells.<sup>4</sup> Doped conjugated polymers exhibit high electronic conductivity and are used, *e.g.*, in the fabrication of chemo- and biosensors,<sup>5</sup> energy storage devices,<sup>6</sup> as hole transporting layers in organic solar cells,<sup>7</sup> and nano-electronics.<sup>8</sup> While most of the current applications utilize the conjugated polymers in bulk or in the form of thin layers, promising applications like ordered heterojunction solar cells<sup>9–11</sup> or single-molecule electronics<sup>12–14</sup> would require

platforms of conductive molecular wires arranged perpendicularly to the surface. In addition, oriented and stretched conjugated polymer chains would significantly improve directional conductivity, which is commonly hindered in bulk or cast films due to the disrupted transport of charge carriers, which have to hop between neighboring chains.<sup>15</sup> Such platforms would also be ideal systems for the investigation of charge transport on the molecular scale, which is a subject of great interest for both practical applications and fundamental understanding of the process.<sup>16–19</sup>

Surface-grafted conjugated polymer brushes with the chains attached by one end to a surface and stretched away perpendicularly to a substrate may address those needs. Polymer brushes can be obtained *via* “grafting from” or “grafting to” approaches.<sup>20</sup> However, only the “grafting from” method enables the formation of very dense brushes with the chains in an extended conformation. The most common polymerization techniques used in the “grafting from” approach are surface-initiated controlled radical polymerizations (SI-CRP)<sup>21–24</sup> which enable control over the brush thickness, composition, architecture and end-functionality. In particular, photoiniferter-mediated polymerization (PMP) introduced by Otsu *et al.*<sup>25</sup> in solution is a versatile method that was used to graft polymer brushes from various substrates.<sup>26–29</sup> This polymerization

Jagiellonian University, Faculty of Chemistry, Ingardena 3, 30-060 Krakow, Poland.  
E-mail: zapotocz@chemia.uj.edu.pl

† Electronic supplementary information (ESI) available: <sup>1</sup>H NMR, <sup>13</sup>C NMR, FTIR and UV/Vis absorption spectra of the monomer; FTIR spectra, contact angle, and ellipsometric measurements of the photoiniferter monolayer. Determination of the thicknesses, UV/Vis absorption spectra, current and adhesion mapping by AFM and XPS measurements of the brushes. AFM topography image of the brushes in water. Experimental results of the investigation of the mechanism of the template polymerization. Calculations of the brush conductivities. See DOI: 10.1039/c4sc04048a



enables spatial and temporal control over the brushes by modifying the irradiation conditions and does not require the addition of any catalysts.

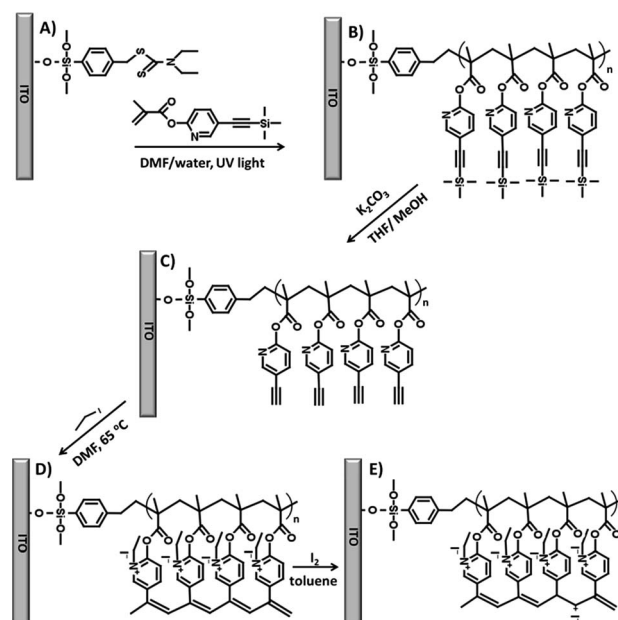
SI-CRP can hardly be used directly for the formation of conjugated polymer brushes since such polymers are generally synthesized by step-growth polymerization. Many attempts, mainly involving organometallic chemistry, have been undertaken to develop alternative methods of formation for surface tethered conjugated polymer chains.<sup>30–38</sup> Such approaches have some constraints related to the chemical functionality of the applied monomers.<sup>39,40</sup> We have only recently proposed the concept of self-templating surface-initiated polymerization (ST-SIP) of bifunctional monomers, which enables the formation of ladder-like conjugated brushes.<sup>41</sup> It is based on the formation of multimonomer template chains in the first polymerization step, followed by the second polymerization leading to conjugated chains in an overall ladder-like architecture.

In the current work we present a versatile synthetic strategy that led to the formation of conjugated polyelectrolyte brushes serving as a platform of high conductivity molecular wires oriented perpendicularly to the surface. To the best of our knowledge, the synthesis of such polyelectrolyte ladder brushes has not been reported yet. They were obtained here by the polymerization of a newly synthesized bifunctional pyridine-based monomer using a catalyst-free quaternization polymerization (QP) in the second step of the ST-SIP approach. QP was originally introduced for ethynylpyridines in solution by Subramanyam and Blumstein<sup>42,43</sup> but has not been applied for surface grafted chains yet. The formation of these conductive chains was realized by means of a simple activation of the pendant acetylene groups aligned along the template chains by quaternization of the attached pyridine rings. Moreover, neither catalysts nor free initiators were needed, so there was no restriction of the surface reactions due to the limited diffusion of such compounds. The formed polymeric nanowires were characterized spectroscopically and using tunneling atomic force microscopy, which enabled the determination of their conductance in the direction perpendicular to the surface.

## Results and discussion

### Surface-initiated photoiniferter-mediated polymerization

A new bifunctional pyridine-based monomer, 5-[2-(trimethylsilyl)ethynyl]pyridin-2-yl 2-methylprop-2-enoate (MTEP) was synthesized and used for the formation of the brushes. It contains a methacryloyl group which can be polymerized by CRP and an acetylenic group which may be subsequently used for the formation of conjugated chains. PMP initiated from the photoiniferter monolayer on an indium tin oxide (ITO) surface was used to polymerize MTEP in the first step, leading to brushes with multimonomer chains (Scheme 1A and B). This controlled polymerization can be easily triggered by UV light, and no additives which could otherwise react with the alkyne groups are necessary. A conductive ITO surface was used here due to the better thermo- and photostability of the polymer



Scheme 1 Scheme of the synthesis of ladder-like conductive ionic polymer brushes. (A) Surface-initiated photoiniferter-mediated polymerization of the MTEP monomer, (B) multimonomer with protected triple bond groups, (C) deprotection step, (D) template polymerization: formation of ladder-like ionic brushes with conjugated polyacetylene chains and (E) iodine doped conductive ionic polymer brushes.

chains tethered to this surface *via* an –O–Si bond compared to the Au–S one formed in the monolayers on gold.<sup>44</sup> Furthermore, ITO substrate is commonly used in the construction of photovoltaic devices, which are a key application of the conductive brushes.

A number of polymerizations were performed with varied reaction times, light powers, and monomer concentrations. While polymer brushes as thick as *ca.* 22 nm were obtained (see Fig. S6<sup>†</sup>), for further studies three samples were chosen with dry thicknesses of 3 nm (PMTEP-3), 5 nm (PMTEP-5), and 7 nm (PMTEP-7), as determined by the AFM scratching method (Table 1 and Fig. S7<sup>†</sup>). Such thin layers allow differences in their electrical conductivity to be shown (see below) and are relevant to their potential applications as hole transporting layers in organic photovoltaics.<sup>30</sup> The formation of the PMTEP-7 brushes was followed by XPS (see ESI<sup>†</sup>) and grazing-angle reflectance FTIR spectroscopy (Fig. 1). The bands characteristic of the pyridine ring (aromatic C–H, 3040–3020  $\text{cm}^{-1}$ ; aromatic C–C, 1592, 1572, 1475  $\text{cm}^{-1}$ ), polymer main chain (aliphatic C–H, 2988–2862  $\text{cm}^{-1}$ ), ester group (C=O, 1766  $\text{cm}^{-1}$ ), and protected acetylene groups (C $\equiv$ C, 2165  $\text{cm}^{-1}$ ), were observed in the IR spectrum of the brushes. No bands characteristic of the C=C vibration at about 1600–1650  $\text{cm}^{-1}$  were observed, confirming that the triple carbon–carbon bonds were not affected under the photopolymerization conditions. The AFM topography measurements of the PMTEP brushes (Fig. 2) indicate that the brushes uniformly cover the surface of the ITO. The formation of the brush layer can be clearly distinguished in the adhesion mapping (Fig. S9<sup>†</sup>).



Table 1 Conditions for SI-PMP of MTEP and the thicknesses of the obtained brushes

Sample	Polymerization time [h]	MTEP concentration [mol dm <sup>-3</sup> ]	Power of the UV lamps <sup>a</sup>	Dry brush thickness [nm]
PMTEP-3	4	0.20	48 W	3.3 ± 0.4
PMTEP-5	20	0.20	24 W	5.0 ± 0.9
PMTEP-7	24	0.23	24 W	7.2 ± 0.9

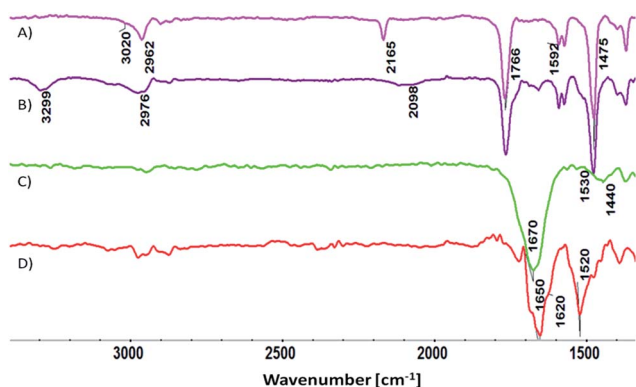
<sup>a</sup> λ<sub>max</sub> = 300 nm.

Fig. 1 Grazing-angle reflectance FTIR spectra of the PMTEP-7 brushes (A), after deprotection of the triple bonds (B), after subsequent template polymerization (C), and after doping of the brushes with iodine (D).

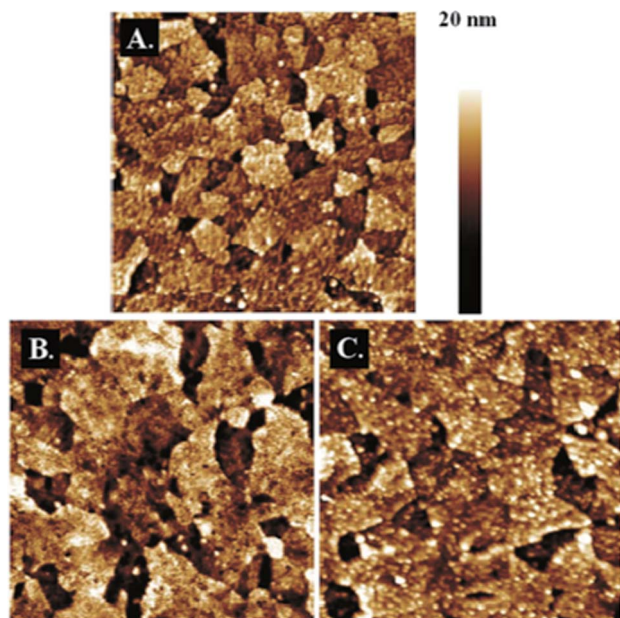


Fig. 2 AFM height images (2 μm × 2 μm) in PFT mode of the clean ITO surface (A), PMTEP-7 before (B) and after QP (C).

### Template quaternization polymerization of PMTEP

After the SI-PMP, the acetylene groups in the multimonomer chains (Scheme 1B) were deprotected by treatment with potassium carbonate solution (Scheme 1C). Successful deprotection

was indicated by the appearance of a band at about 3300 cm<sup>-1</sup> in the FTIR spectrum that may be assigned to the C–H vibration of the terminal acetylene group (Fig. 1B). Furthermore, the band at 2165 cm<sup>-1</sup> (Fig. 1A), assigned to C≡C vibrations, was shifted to 2098 cm<sup>-1</sup>. This band is characteristic of the terminal acetylene group and was observed in ethynylpyridine monomers.<sup>42</sup> Moreover, the band assigned to aliphatic C–H vibrations shifted slightly due to the disappearance of the trimethylsilyl groups in the brushes. All these changes confirmed the complete deprotection of the acetylene groups.

Finally, the deprotected acetylene groups in the multimonomer chains were polymerized using template polymerization (Scheme 1D). This was accomplished by simple quaternization of the pyridine rings using ethyl iodide. After QP the bands at 3300 cm<sup>-1</sup> and 2098 cm<sup>-1</sup> completely disappeared from the FTIR spectrum (Fig. 1C) indicating polymerization of the acetylene groups. In addition, a very strong and broad band at about 1670 cm<sup>-1</sup> appeared in the spectrum. This band may be assigned to the formed pyridinium salt with contribution from the bands assigned to the carbonyl group (shifted) and the conjugated polyacetylene chain (shoulder at 1600–1650 cm<sup>-1</sup>), as previously reported for similar polymers obtained in solution.<sup>42</sup> A relatively high effective conjugation length<sup>45</sup> in the obtained brushes is also indicated in the measured UV/Vis spectrum (see Fig. S8†) which is significantly red-shifted (λ<sub>max</sub> ≈ 570 nm) compared to those typically reported for ionic poly(ethynyl pyridines) synthesized in solution (rarely exceeding 500 nm).<sup>42</sup> This may be the consequence of a more extended conformation of the chains in the brushes compared to the situation in solution.

Some nanometer sized features appeared in the AFM image of the brushes after QP (Fig. 2C). This may indicate some stiffening of the formed brushes due to the formation of the conjugated chains or partial bridging of the neighboring chains (see further). It is worth mentioning that the brushes swell in water (see Fig. S11†) due to the presence of the charged groups along the chains. Repulsion between those groups located along the chains leads to their further stretching, and intermolecular repulsion should prevent bridging of the neighboring chains.

The obtained ladder-like polymer brushes were subsequently doped with iodine (Scheme 1E). The FTIR spectrum of the brushes after doping (Fig. 1D) exhibited some shifting of the C=C band from 1670 cm<sup>-1</sup> to 1650 cm<sup>-1</sup>, which may indicate changes related to the doping of the conjugated chain that influence the neighboring pyridine rings. In addition, the intensity of this band significantly decreased with respect to the



band assigned to the conjugated chain that now appears as a clear shoulder at *ca.* 1620  $\text{cm}^{-1}$ .

### Mechanism of the template quaternization polymerization in the brushes

In order to verify the originally proposed mechanism of the QP<sup>42</sup> of the 2- and 4-ethynylpyridines and their derivatives in solution, some additional experiments were performed for the brushes (see ESI<sup>†</sup>). Based on the obtained results it may be concluded that the previously proposed hypothesis on initiation of QP by the counter ions is not applicable in the current system. Instead, a free electron pair at the nitrogen atom of the pyridine seems to play a key role in the initiation process. Thus, the presence of non-quaternized nitrogen atoms in the grafted chains is crucial to start the QP of the acetylene groups. Therefore, taking also into account the previous studies on the polymerization of monosubstituted ethynylpyridines in solution<sup>46</sup>, we could propose the mechanism of the template polymerization in the brushes (see Scheme 2). The initiation step involves quaternization of the pyridine ring, which activates the attached acetylene group, followed by the nucleophilic attack of the nitrogen atom with a free electron pair on the activated acetylene groups (bound to the quaternized pyridines). As a result a carbanion is formed on the acetylene group which may react with a neighboring monomer unit, leading to the formation of the conjugated chain. Thus, the chains may be formed by the groups located along the same template chain or with a contribution of the groups from the neighboring chains (which is less likely since the chains are separated due to electrostatic repulsions). Moreover, problems related to the inhomogeneity of brushes subjected to post-polymerization treatment with external reagents are in this case very limited, as only small molecules of ethyl iodide have to diffuse to the chains and activate the acetylene groups.

### Electrical properties of the brushes

The doped conjugated PMTEP brushes were found to be highly conductive, as shown using tunneling AFM (tuna-AFM) mapping (Fig. 3) and by collecting current-voltage (*I-U*) plots (see Fig. S14<sup>†</sup>) using the same technique in the spectroscopic mode. The good electrical contact required between the conductive AFM tip and the brush surface usually implies the application of relatively high loads on the AFM cantilever.

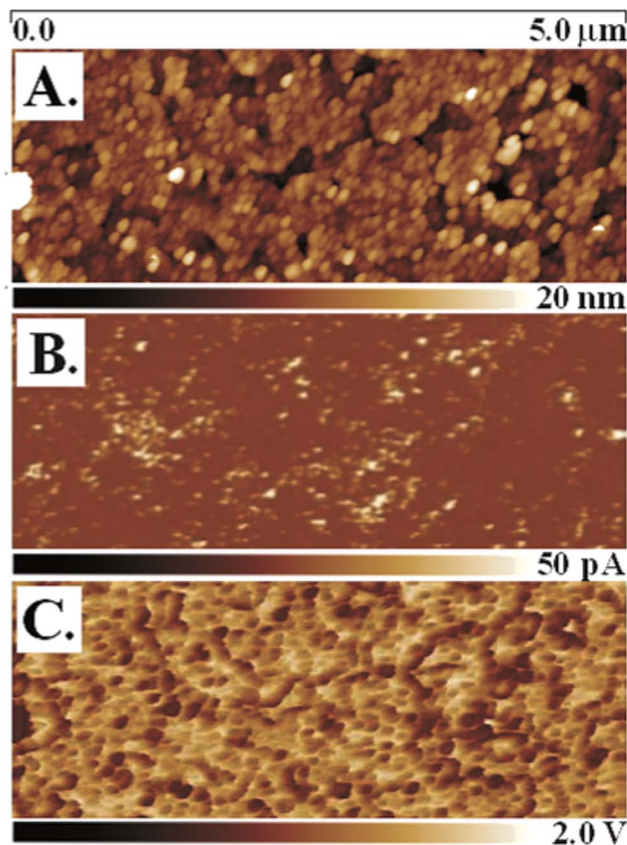
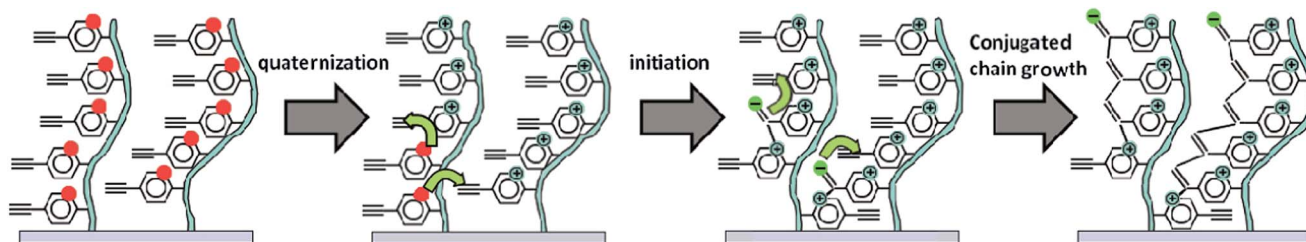


Fig. 3 Tuna-AFM mapping of the doped PMTEP-7 brush: (A) topography image, (B) current map at 25 mV DC sample bias, (C) adhesion map.

However, for soft polymer brushes, especially low external loads should be applied in order not to push the tip through the brushes down to the ITO surface. Thus, all the experiments were performed using tuna Peak Force Tapping (PFT) mode, which enables control over the external load (which was kept close to zero, <20 pN) during current measurements. The current map of the doped brushes (Fig. 3B) exhibits randomly distributed spots indicating high conductance, which is in line with homogenous coverage of the brush surface (Fig. 3A). The adhesion map (Fig. 3C) also supports homogenous distribution of the brushes on the surface without the presence of loosely bound deposits from the solution that would produce higher local contrast in the adhesion map. There is some spatial correlation between the high current and high



Scheme 2 Proposed mechanism of the template QP of the brushes.



adhesion spots observed, but topography convolution in the current image seems to be absent (Fig. S10†). This can be explained by the similar dependences of current and adhesion on the tip-surface contact area. It is also clear that at an external load near zero a good electrical contact between the tip and the brushes may be formed only due to attractive adhesive forces.

Conductivity measurements at the nanoscale in the studied system rely on the electrical contact between the AFM tip and the conjugated part of the ladder-like brushes. This contact may vary from one curve to another as the conformations of the chains in the brushes are statistically distributed both in space and time. This also implies a broad distribution of the measured conductance ( $dI/dU$ ) values for the studied brushes (Fig. 4C–E). Variations of the adhesion forces that influence the actual contact area between the tip and surface and the possibility of its temporal contamination may also contribute to broadening of the distribution.

Nevertheless, for the shortest brushes (PMTEP-3) the conductance was found to be very large, on the level of  $10^3$  to  $10^4$   $\text{pA V}^{-1}$  (Fig. 4C). The value at the maximum of the histogram is even larger than for bare ITO (Fig. 4A) since the effective contact area should be larger in the case of the pliable polymer brushes than stiff ITO.<sup>47</sup> It is worth mentioning that the values of conductance obtained for ITO ( $10^3$ – $10^4$   $\text{pA V}^{-1}$ ) resulted in its conductivity on the level of  $10^6$   $\text{S m}^{-1}$ , which correlates very well with the literature values.<sup>48</sup> Additionally, the histogram for ITO is much narrower than the one for PMTEP-3, as contact between two solid surfaces may be established in a more reproducible

manner. However, in order to rule out a possible short circuit between the tip and the supporting ITO surface in the case of the doped PMTEP-3 brushes, we have performed the same conductivity measurements for non-doped PMTEP and nonconductive PNIPAM brushes of similar height ( $\approx 3$  nm). As can be judged from the histogram (Fig. 4B), the PNIPAM layer effectively blocks current flow as the majority of the curves showed no or very little conductance (some high conductance events observed in the histogram of PNIPAM may be the result of establishing some contacts with ITO surface). Qualitatively the same results were obtained for non-doped PMTEP-3. Thus, it is clear that the measured conductance for the doped PMTEP-3 sample should be assigned to the conductive brushes themselves (some contribution of ITO cannot be excluded). Based on the measured  $dI/dU$  values one may estimate the specific conductance for the doped brushes to be in the range  $10^{-1}$ – $10^0$   $\text{S m}^{-1}$  (see ESI†), which is several orders of magnitude higher than those measured for similar iodine doped poly(ethynylpyridine)s synthesized in solution ( $10^{-6}$ – $10^{-5}$   $\text{S m}^{-1}$ ).<sup>42,43</sup> It seems that the orientation of the conjugated macromolecules plays a key role in the efficient transport of charge carriers. Such high conductance may be explained by the elongated conformation of the chains in the brushes and the high effective conjugation length, leading to directional charge transport along single macromolecules that cannot be realized in bulk. Even if some bridging between the neighboring chains after QP cannot be excluded, the conjugation may still be preserved, enabling efficient electron flow along the chain (Scheme 3). Importantly, in such brushes sandwiched between the AFM tip and ITO surface, intramolecular charge transport may be dominant over intermolecular hopping, which is the factor limiting the bulk conductivity of conjugated polymers.

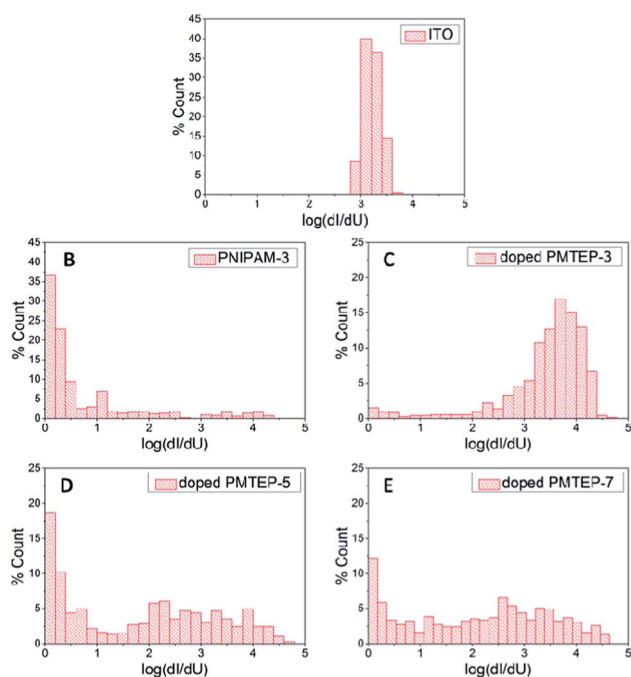
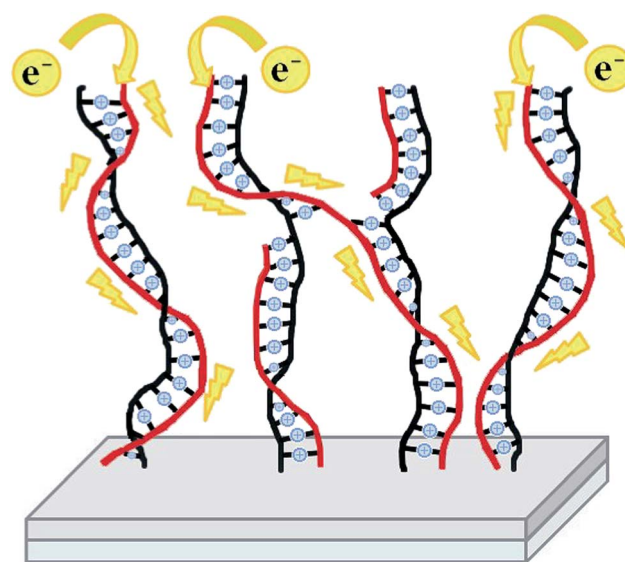


Fig. 4 Histograms of  $dI/dU$  values collected for: (A) native ITO, (B) nonconductive PNIPAM brushes on an ITO surface, (C) doped PMTEP-3 brushes, (D) doped PMTEP-5 brushes and (E) doped PMTEP-7 brushes.



Scheme 3 Schematic representation of the ladder-like conjugated brushes grafted from a surface and directional electron flow along the conjugated chains.



For the taller brushes, PMTEP-5 and PMTEP-7, the distribution of the conductance values is much broader compared to that of PMTEP-3. This is not surprising since more variations in establishing tip-brush contact are possible for longer chains. In addition, the level of doping may vary locally, and breaking of the conjugation along the brush chains is more likely for longer chains. Nevertheless, the majority of the curves exhibited conductance values in the range of  $10^1$  to  $10^4$  pA  $V^{-1}$ , which results in a conductivity in the range of  $10^{-3}$  to  $10^0$  S  $m^{-1}$ , which is still much larger than the values reported for similar polymers in bulk.

## Conclusions

We applied here the concept of self-templating surface-initiated polymerization to the synthesis of ionic conjugated polymer brushes serving as surface-grafted molecular wires. A newly synthesized bifunctional monomer was used in the controlled photoiniferter-mediated polymerization, resulting in the formation of multimonomer surface-grafted chains with polymerizable ethynylpyridine pendant groups. Those groups aligned along the template chains were subsequently polymerized using catalyst-free quaternization polymerization, leading to charged ladder-like brushes with conjugated poly(ethynylpyridine) chains. After doping with iodine, the brushes exhibited high conductivity ( $10^{-1}$  to  $10^0$  S  $m^{-1}$  for the shortest chains) in the direction perpendicular to the surface as determined using tuna-AFM. Brushes of various heights were prepared and their electrical conductance was found to decrease with increasing brush height. Even so, the obtained conductivity values were several orders of magnitude higher than those measured for similar polymers in bulk, which emphasizes the importance of the ordering of the chains for the electrical performance of the polymer layers. Due to their relatively long conjugation and ionic nature, these brushes have potential as materials for mixed ionic and electronic conductivity, suitable for energy storage or photovoltaics applications. The proposed approach is very versatile as various polymerizable groups forming conjugated chains may be aligned along the templates and form conductive polymers. The proof of concept of ST-SIP presented here may be easily extended to other relevant surfaces and polymerizable side groups and is easily adaptable for soft lithographic techniques. The formation of conjugated brushes of various architectures (e.g., block conjugated brushes, mixed brushes, gel brushes) is straightforward using this approach. This synthetic approach offers great tunability in the properties of the brushes by changing the chemistry of the monomer, the nature of the quaternizing agent, or the type of counterion used. Importantly, conjugated chains with the ladder-like architecture seem to be less prone to electrical instabilities compared to conventional conductive layers based on polymeric materials, as the tuna-AFM measurements here were performed at ambient conditions. The presented method of fabrication of conductive molecular wires oriented perpendicularly to the surface may significantly contribute to the development of molecular electronics and photovoltaics.

## Acknowledgements

The authors would like to thank the Polish Ministry of Science and Higher Education for the financial support ("Ideas Plus" grant no. IdP2011 000561). The P2M program from the ESF is also acknowledged. The authors also thank A. Bernasik and M. Wyrwał (ACMiN AGH, Krakow) for performing XPS measurements.

## Notes and references

- 1 H. Shirakawa, E. J. Louis, A. G. MacDiarmid, C. K. Chiang and H. J. Heeger, *J. Chem. Soc., Chem. Commun.*, 1977, **16**, 578.
- 2 Y. H. Kim, J. Lee, S. Hofmann, M. C. Gather, L. Müller-Meskamp and K. Leo, *Adv. Funct. Mater.*, 2013, **23**, 3763.
- 3 H. Sirringhaus, *Adv. Mater.*, 2014, **26**, 1319.
- 4 L. Dou, J. You, Z. Hong, Z. Xu, G. Li, R. A. Street and Y. Yang, *Adv. Mater.*, 2013, **25**, 6642.
- 5 J. Liang, K. Lia and B. Liu, *Chem. Sci.*, 2013, **4**, 1377.
- 6 Y. Qiao, M. S. Islam, K. Han, E. Leonhardt, J. Zhang, Q. Wang, H. J. Ploehn and C. Tang, *Adv. Funct. Mater.*, 2013, **23**, 5638.
- 7 H. Zhou, Y. Zhang, C.-K. Mai, S. D. Collins, T.-Q. Nguyen, G. C. Bazan and A. J. Heeger, *Adv. Mater.*, 2014, **26**, 780.
- 8 Y.-Z. Long, M.-M. Li, C. Gu, M. Wan, J.-L. Duvail, Z. Liu and Z. Fan, *Prog. Polym. Sci.*, 2011, **36**, 1415.
- 9 F. S. Kim, G. Ren and S. A. Jenekhe, *Chem. Mater.*, 2011, **23**, 682.
- 10 N. Yeh and P. Yeh, *Renewable Sustainable Energy Rev.*, 2013, **21**, 421.
- 11 S. Zhang, C. I. Pelligra, G. Keskar, J. Jiang, P. W. Majewski, A. D. Taylor, S. Ismail-Beigi, L. D. Pfefferle and C. O. Osuji, *Adv. Mater.*, 2012, **24**, 82.
- 12 Y. Okawa, M. Akai-Kasaya, Y. Kuwahara, S. K. Mandala and M. Aono, *Nanoscale*, 2012, **4**, 3013.
- 13 C.-A. Palma and P. Samori, *Nat. Chem.*, 2011, **3**, 431.
- 14 H. Song, M. A. Reed and T. Lee, *Adv. Mater.*, 2011, **23**, 1583.
- 15 M. Alonzi, D. Lanari, A. Marrocchi, C. Pietrucci and L. Vaccaro, *RSC Adv.*, 2013, **3**, 23909.
- 16 L. Luo, S. H. Choi and C. D. Frisbie, *Chem. Mater.*, 2011, **23**, 631.
- 17 H. Hayashi, A. Sobczuk, A. Bolag, N. Sakai and S. Matile, *Chem. Sci.*, 2014, **5**, 4610.
- 18 E. Leary, M. T. Gonzalez, C. van der Pol, M. R. Bryce, S. Filippone, N. Martín, G. Rubio-Bollinger and N. Agraiöt, *Nano Lett.*, 2011, **11**, 2236.
- 19 L. Lafferentz, F. Ample, H. Yu, S. Hecht, C. Joachim and L. Grill, *Science*, 2009, **323**, 1193.
- 20 R. Barbey, L. Lavanant, D. Paripovic, N. Schüwer, C. Sugnaux, S. Tugulu and H.-A. Klok, *Chem. Rev.*, 2009, **109**, 5437.
- 21 Y. Tsujii, K. Ohno, S. Yamamoto, A. Goto and T. Fukuda, *Adv. Polym. Sci.*, 2006, **197**, 1.
- 22 C. M. Hui, J. Pietrasik, M. Schmitt, C. Mahoney, J. Choi, M. R. Bockstaller and K. Matyjaszewski, *Chem. Mater.*, 2014, **26**, 745.



- 23 J. E. Poelma, B. P. Fors, G. F. Meyers, J. W. Kramer and C. J. Hawker, *Angew. Chem., Int. Ed.*, 2013, **52**, 6844.
- 24 J. Yan, B. Li, B. Yu, W. T. S. Huck, W. Liu and F. Zhou, *Angew. Chem., Int. Ed.*, 2013, **52**, 9125.
- 25 T. Otsu and M. Yoshida, *Makromol. Chem. Rapid Commun.*, 1982, **3**, 127.
- 26 E. M. Benetti, S. Zapotoczny and G. J. Vancso, *Adv. Mater.*, 2007, **19**, 268.
- 27 S. B. Rahane, S. M. Kilbey and A. T. Matters, *Macromolecules*, 2005, **38**, 8202.
- 28 B. de Boer, H. K. Simon, M. P. L. Werts, E. W. van der Vegte and G. Hadziioannou, *Macromolecules*, 2000, **33**, 349.
- 29 X. Sui, S. Zapotoczny, E. M. Benetti, M. Memesa, M. A. Hempenius and G. J. Vancso, *Polym. Chem.*, 2011, **2**, 879.
- 30 L. Yang, S. K. Sontag, T. W. La Joie, W. Li, N. E. Huddleston, J. Locklin and W. You, *ACS Appl. Mater. Interfaces*, 2012, **4**, 5069.
- 31 S. K. Sontag, N. Marshall and J. Locklin, *Chem. Commun.*, 2009, 3354.
- 32 N. Marshall, S. K. Sontag and J. Locklin, *Chem. Commun.*, 2011, **47**, 5681.
- 33 B. Yameen, C. Rodriguez-Emmenegger, C. M. Preuss, O. Pop-Georgievski, E. Verveniotis, V. Trouillet, B. Rezek and C. Barner-Kowollik, *Chem. Commun.*, 2013, **49**, 8623.
- 34 A. Bousquet, H. Awada, R. C. Hiorns, C. Dagron-Lartigau and L. Billon, *Prog. Polym. Sci.*, 2014, **39**, 1847.
- 35 N. Khanduyeva, V. Senkovsky, T. Beryozkina, M. Horecha, M. Stamm, C. Uhrich, M. Riede, K. Leo and A. Kiriy, *J. Am. Chem. Soc.*, 2009, **131**, 153.
- 36 N. Doubina, J. L. Jenkins, S. A. Paniagua, K. A. Mazzio, G. A. MacDonald, A. K.-Y. Jen, N. R. Armstrong, S. R. Marder and C. K. Luscombe, *Langmuir*, 2012, **28**, 1900.
- 37 S. Kang, R. J. Ono and C. W. Bielawski, *J. Am. Chem. Soc.*, 2013, **135**, 4984.
- 38 D. F. Zeigler, K. A. Mazzio and C. Luscombe, *Macromolecules*, 2014, **47**, 5019.
- 39 A. Kiriy, V. Senkovskyy and M. Sommer, *Macromol. Rapid Commun.*, 2011, **32**, 1503.
- 40 Z. J. Bryan and A. J. McNeil, *Macromolecules*, 2013, **46**, 8395.
- 41 M. Szuwarzyński, J. Kowal and S. Zapotoczny, *J. Mater. Chem.*, 2012, **22**, 20179.
- 42 S. Subramanyam and A. Blumstein, *Macromolecules*, 1991, **24**, 2668.
- 43 S. Subramanyam, A. Blumstein and K. P. Li, *Macromolecules*, 1992, **25**, 2065.
- 44 J. J. Gooding and S. Ciampi, *Chem. Soc. Rev.*, 2011, **40**, 2704.
- 45 H. Meier, U. Stalmach and H. Kolshorn, *Acta Polym.*, 1997, **48**, 379.
- 46 L. Balogh and A. Blumstein, *Macromolecules*, 1995, **28**, 25.
- 47 A. Kovalev, H. Shulha, M. Lemieux, N. Myshkin and V. V. Tsukruk, *J. Mater. Res.*, 2014, **19**, 716.
- 48 A. K. Kulkarni, K. H. Schulz, T. S. Lim and M. Khan, *Thin Solid Films*, 1999, **345**, 273.

